

### **Anonymous Referee #1**

This manuscript describes the results of surveys of eggs and larvae south of Sicily in the summers of contrasted years 2010 and 2011. Differences in distribution, especially between Capo Passero and Malta, are attributed to differences in wind forcing resulting in a stronger offshore filament in 2010; the filament would advect larvae from the Cape to Malta. The attribution seems logical enough, and there is some back-up from Lagrangian modelling, although with only two cases one cannot be sure about the possible role of other factors not discussed here. The interest is rather limited, because the study is geographically localised and there is nothing particularly novel about the techniques used. It can have its place in the context of other papers in the region.

Many thanks for the positive and encouraging comment. We are aware of the fact that our analysis is geographically localized. However, we believe that this should not be considered as a limitation. From a marine biology perspective, motivations for conducting a Lagrangian connectivity analysis, like the one presented in this ms, may come even from regional areas, where it can be relatively easier to establish dynamical connections across the domain. On the other hand, every sub-basin may present its peculiarities, from a physical oceanography point of view, so that it is not obvious that extending the study to wider domains corresponds to gain in physical information, proportionally. Said that, in the revised version we stress how our findings (since supported by a general theory) can be applied to similar geographical regions where fate and distribution of small pelagic fish larvae are potentially affected by wind effects [See line 326-328]. Regarding the novelty of our technique, we point out that nobody else (with the exception of some co-authors of this ms in recent publications), to our knowledge, uses kinematic models of mesoscale turbulent dispersion coupled to a large-scale ocean circulation model. The use of a generic kinematic eddy model (i.e., a “kinematic simulation”) does not guarantee an accurate numerical simulation of Lagrangian turbulent trajectories in a regime where the locality hypothesis for particle dispersion is expected to hold (see Thomson and Devenish, 2005, for a critical discussion about the use of kinematic simulations of turbulence). Our kinematic model fulfills the basic theoretical requirements for this scope (see Lacorata et al., 2008 or Lacorata et al., 2014 for a full description of the method) and has the advantage to be suitable for any kind of scaling regime (the Richardson’s law is only an example). See line 151-187.

However, it does need considerable improvement in the description of what was actually done, particularly in respect of the models used.

We fully agree with this comment. In this revised version, as mentioned above, we improve the part dedicated to the description of our numerical simulations and the novelty of our technique. See line 151-187.

I think the authors should also consider the difference between years in terms of the direct wind forcing (leading to upwelling and possibly a filament off Capo Passero) as well as the wind-stress curl.

We actually performed such an analysis (Figure 6). In the revised version of the ms, however, we discuss with more details the role of Ekman transport (i.e., wind forcing and upwelling induce currents) and we explain

better the link between this and the wind-stress curl (i.e., input of Potential Vorticity that triggers the offshore evolution of the filament). See line 222-236; 260-267; 270-298.

There are many places where the English usage should be improved, but much of this could be through the final copy-editing

English language has been carefully revised.

Page 2098. Line 12. "use" not "hire". Lines 17-18. Does "more favourable" refer to Capo Passero in 2011 or Malta in 2010? Line 19. Omit "want to".

Thanks of these corrections. We now specify that the more favorable condition is represented by an alongshore transport towards the recruiting area of Capo Passero. See Line 28-30.

Page 2099. Line 9. "pelagic fish"? "pelagic" is an adjective and needs to be followed by a noun, e.g. "fish". Line 13 should read ". . sea, i.e. E. encrasicolus . .". Line 23. "of" or "on"? At present with "of" this means effect of fish catch on abundance and northward expansion. Use "on" if you mean effect of abundance on fish catch.

Thanks. We corrected all these sentences.

Page 2100. Line 1. "chlorophyll-enriched". Line 4. "pelagic fish" as above? Line 7. Put ". . ." around "connect the dots". Lines 8-9. Not "i.e."; the central Mediterranean is not the same as the Sicily Channel. Either ". . central Mediterranean Sea and specifically the Sicilian Channel. . ." or omit "central Mediterranean Sea (i.e.". Lines 17-19. I don't think the current is due to upwelling, especially if "This current often gives rise to the cold filament." I think the wind causes both the current and the upwelling.

Thanks for these corrections. We modified these sentences accordingly and, in particular, we clarified the sentence related to the cold filament. See line 78-87

Page 2101. Line 2. Any initial hypothesis should be stated in the introduction. If it only follows from the results, is it a hypothesis? Line 12. Insert "further" before "offshore". Line 16. "hauled from within 5m of the bottom . .". Lines 16-17. ". . at deep stations . .". Line 17. Omit "on". Line 21. Not "at binocular". Do you mean "under a microscope"?

Thanks, we made all the suggested corrections. Regarding page 2101 Line 2 we have slightly changed the sentence. Indeed we believe that Lagrangian simulations have to be considered as numerical experiments that can be designed either to test an old hypothesis or to find out hints for a new one. In our case we want to verify the relationship between wind forcing, upwelling events, and Lagrangian transport variability. This

framework allows us to reinforce the initial hypothesis and to pursue the potential vorticity analysis that, consequently, provides a mechanistic explanation regarding the link between wind effects and offshore transport of larvae. [See line 97-99.](#)

Page 2102. Line 4. Better “. . In particular, eggs were assigned a stage number”. Line 5 end. “following”. Lines 9, 11. Move “were obtained” from end of sentence to after “(TL, mm)”. Line 11. Better “. . Then length classes at 1 mm intervals were”. Lines 25, 26. Surely the wind stress does not suddenly decrease at 11 m/s.

Thanks, we made all corrections.

Page 2103. Section 2.3 is unclear and needs to say what was actually done. What is the main model? Its area (figures 3 and 4 show different extent)? Resolution? Open boundary conditions and forcing? Period(s) run? Line 13. “instances” seems the wrong word – is it referring to (i) and (ii)? Line 14. “scope” seems the wrong word – I cannot tell what it refers to. Lines 17-18. This implies that the total velocity is made up of such cells. Surely they are added to a larger-scale deterministic velocity (where from)?

Thanks for this remark. This section has been revised by specifying the following information. The main model is the Ocean model provided by the Mediterranean Forecasting System (see, e.g., Tonani et al., 2008, for a detailed description of the Ocean model that is not necessary to repeat here). The Ocean model covers all the Mediterranean basin. Horizontal and vertical spatial resolution are, respectively,  $1/16 \times 1/16$  degree (6.5 km) and 72 vertical layers ranging from 1.5 m to 5000 m depth. Daily re-analysis velocity fields are used for the large-scale circulation while a 2D kinematic eddy field and a 3D convective cell field are added to the main model to compensate the lack of, respectively, effective mesoscale turbulent dispersion and vertical mixing in the mixed layer (see Palatella et al., 2014, and Lacorata et al., 2014, for more details about this type of modelling techniques). The boundary conditions are open (if meant relative to the Sicily Channel sub-domain), with rebound conditions of the Lagrangian particles against the coasts (an accurate modelling of the circulation in proximity of coastal boundaries is outside the capabilities of the Ocean model we have used). Wind forcing is provided by ECMWF data every six hours. Period of the simulation: from June, 1st to September, 30th for 2010 and 2011. All other corrections have been made and, moreover, we have specified where the larger-scale deterministic velocity field comes from: the total velocity in a given point is the sum of the Ocean model velocity (i.e. the MFS model) plus the kinematic model(s) velocity. [See line 151-187](#)

Line 13. “instances” seems the wrong word – is it referring to (i) and (ii)? Line 14. “scope” seems the wrong word – I cannot tell what it refers to.

We changed “both instances” with “these drawbacks”. We also changed “Deterministic chaotic flows work...etc...(Palatella et al., 2014)” with “Deterministic chaotic flows are very suitable, at this regard, since they can generate trajectories that accurately (in statistical terms) simulate the typical small-scale turbulent motions that affect the dispersion of a tracer distribution at early stage (Palatella et al., 2014).” [See line 170-187.](#)

Page 2104. Lines 3-6. Are these sentences describing previous work or results of the present study? Line 9. Better “. . . was greater than in 2011 . . .”. Line 11. “. . . The abundances differed between . . .”? Line 14. Better “Analysis of egg stages revealed different spatial distributions . . .”. Line 21. “. . . eggs were found . . .” (“exclusively” is redundant; “only” already gives the meaning). Line 23. Omit “was”. Line 26. “length” not “dimensional” – say what you mean. Also page 2105 line 2, page 2108 line 21. Line 27. “9” not “8”?

Thanks, we made all corrections. Regarding Section 3.1, the old line 3-6 (page 2104) refers to our results in this present study. There are no previous works that describe the spawning pattern in this specific area. [See the new line 194-204.](#)

Page 2105. Line 1. Omit “more”. Lines 2-3. “. . . we recorded very few larvae.” (see figure 2, there is at least one). Line 6. “. . . a smaller length range . . .”. Line 8. Omit “coastal, upwelling induces” (as above). Line 13. “. . . filament generated off Capo . . .”. Section 3.2 The timings of the model results need to be treated carefully to be relevant to the cruise dates.

Thanks, we made all corrections. In Section 2.3 we spend some words regarding the timings of the model. Buoyant particles of the Lagrangian runs are emitted at constant rate in the period from June, 1st to September, 15<sup>th</sup> (for both years). So the dates we mentioned are consistent with the cruise samplings. [See line 165-168.](#)

Page 2106. Line 2. Where do these Eulerian velocity fields come from – what model run exactly? Line 20. “. . . in 2010, when the Mistral wind blew steadily for”.

Thanks, we made all corrections. We make clear that the Eulerian velocity fields are from the Ocean model provided by the Mediterranean Forecasting System (Tonani et al., 2008). [See line 151-169.](#)

Page 2107. Line 1. “along . . . filament.” I do not understand this. Line 3. “. . . we use a surface cold filament model”. Rest of section. How does the effect of wind stress curl compare with the effect of the wind-forced coastal current and coastal upwelling? The supplementary figure S4 seems to show rather strong offshore Ekman transport on a few days. Line 19. Add “,” after “model”.

Thanks, we made all corrections. We now explain the link among the curl of wind stress, the wind-induced coastal current, and the coastal upwelling. We here use the PV model as a diagnostic tool to quantify the efficiency of the cold filament in delivering eggs and larvae offshore. Surely, the cold filament is generated by the coastal upwelling. However, the analysis of the wind stress curl quantifies the PV input that is needed to trigger the offshore evolution of the filament. [See lines 222-236; 263-267; 270-273; 294-298.](#)

Figure 5c should show 2011

The figure is now correct. Thanks and sorry for the mistake.

All the other minor comment were fully addressed

### **Anonymous Referee #2**

Figure 1 is possibly misleading because the dots showing the location of the sampling stations can be confused with the dots showing the abundance of larvae.

Thanks for this comment. We modified this figure.

Also, the distribution appears very patchy, with concentrations at neighboring locations having little in common. Therefore, the real distribution is clearly undersampled and possibly gives a biased view of the real distributions. To gain confidence in the experimental data, more should be said about the total volume of water filtered at the different stations.

Thanks for this comment. In section 3.1 we remark that the distribution of eggs and larvae largely varies among sampling stations due to the spawning behavior of the adults. Indeed, as other small pelagic fish (e.g. *Sardina plichardus* or *Engraulis encrasicolus*), *Sardinella aurita*, spawns in a very localized areas during a brief lapse of time, generating a very patchy distribution within the study area. [See line 191-193](#).

Very little is said about the actual lagrangian method and the numerical set-up. Section 2.3 gives general comments, references but does not provide any information about the real method used in this study.

We fully revise Section 2.3 by specifying the following information:

1) Method: we integrate numerically the evolution of Lagrangian trajectories in an Ocean model (i.e. the MFS model defined in the whole Mediterranean basin) to which a couple of supplementary kinematic velocity fields are added, in order to account for mesoscale turbulent dispersion, on one hand, and a basic vertical mixing in the mixed layer, on the other one. The role of the small-scale kinematic models of dispersion is to fit the numerical simulations of particle transport to observation, at least in terms of characteristic temporal and spatial scales (see for ex. Lacorata et al., 2014, or Palatella et al., 2014). This method is different from the common techniques that are based on the use of stochastic diffusion models (see Thomson 1987 and a plenty of other literature on this). Our kinematic modelling technique is based on deterministic chaos, namely chaotic Lagrangian trajectories generated by simple periodic velocity fields (essentially, multi-scale cellular patterns) to which specific space-time relationships can be assigned.

2) Velocity fields: the total velocity field applied to a Lagrangian particle, in a given point of the domain, is the sum of the Ocean model velocity field (MFS, i.e. the large-scale circulation model) plus the kinematic velocity field. The large-scale Ocean model is provided by the Mediterranean Forecasting System (MFS) in terms of daily output of reanalysis fields. Horizontal and vertical spatial resolution are, respectively, 1/16 x 1/16 degree (6.5 km) and 72 vertical layers ranging from 1.5 m to 5000 m depth. Details about the set up of the additional kinematic models can be found in Lacorata et al. (2014), and Palatella et al., (2014).

3) Buoyancy: numerical simulations assume neutrally buoyant passive particles.

4) Seeding strategy: 25600 particles at constant rate from June 1st to September 15th

5) Timespan: from June 1st to September 30th, 2010 and 2011.

See line 151-187.

Also, the strong statements made at lines 11-14 about the issues related to Lagrangian techniques should be substantiated with appropriate references or omitted.

We believe that these are general and objective considerations: no model has infinite resolution and therefore there will always be issues related to the scales of motion of the order of the grid step, and lesser. The same holds for the vertical motion in a coarsely resolved mixed layer. These drawbacks can be surely mitigated in sophisticated high-resolution models but not totally eliminated. In our case, we use a large-scale circulation Ocean model in order to study Lagrangian transport and dispersion (within a relatively large area). In dealing with finite resolution issues at a mesoscale (and lesser) level, we overcome such an issue by means of our kinematic modelling technique. In the revised version of Section 2.3 we stress this concepts in a clearer way.

See line 170-187.

Please explain the sentence "This indicates that *Sardinella aurita* larvae did not find the ideal dynamics conditions (where ?) for a local recruiting and were delivered offshore". Please also clarify the scenario described on page 2105 (lines 8-13). Obviously, eggs are hatched near Capo Passero. Then, I do not understand how a coastal upwelling can induce a current transporting the eggs along the Sicilian coast and mix (? – current do not mix water masses) these eggs with in situ (where ?) spawning eggs when no eggs are found along the coast...Also why would only larvae larger than 8 mm be advected by the cold filament ?

Sorry, This paragraph was actually really confusing (and some parts were wrong). We now formulate our statements in a clearer and analytic way. See line 222-236.

Figure 3 and 4 do not support the idea of a transport of eggs/larvae from Capo Passero region to the western part of Malta: the main stream flows eastward of Malta. The arrow on figure 3 does not reflect the results of the Lagrangian simulation. It is therefore misleading.

This comment is not really clear. The arrow enlightens a particular branch of the Lagrangian particle trajectories that delivers a large amount of them to the east side of Malta around the 8<sup>th</sup> of July. We do not mention within the text the western part of Malta. Moreover, this is strongly supported by the Eulerian field (which is cruised averaged, and not a single snapshot) that shows the presence of a preferential path from Capo Passero to Malta in 2010 that does not occur in 2011. The reviewer can notice that July 2011 is characterized by weak currents (Fig. 4) and thus particles show a huge dispersion rather than a strong advection towards Malta. We now provide a clearer description of those results in [line 243-249](#).

Figure 5 shows rather different Chl-a content in 2010 and 2011. Therefore, one cannot rule out the fact that the different distributions of *Sardinella aurita* might be due to different temperature conditions (a corrected figure 5c would help) and food web dynamics rather than the occurrence or not of cold filaments transporting eggs and larvae offshore.

Figure 5 has been corrected. Food web dynamics are very unlikely since larvae behave like passive, advected particles. [See line 303-309](#).

# 1 Wind forcing and fate of *Sardinella aurita* eggs and larvae in the 2 Sicily Channel (Mediterranean Sea)

3 Marco Torri<sup>1,4</sup>, Raffaele Corrado<sup>2</sup>, Federico Falcini<sup>3</sup>, Angela Cuttitta<sup>1</sup>, Luigi Palatella<sup>2</sup>, Guglielmo  
4 Lacorata<sup>2</sup>, Bernardo Patti<sup>3</sup>, Marco Arculeo<sup>4</sup>, Salvatore Mazzola<sup>1</sup>, and Rosalia Santoleri<sup>3</sup>.

5  
6 [1] {Istituto per l'Ambiente Marino Costiero, Consiglio Nazionale delle Ricerche, Capo Granitola (TP), Italy}

7 [2] {Istituto di Scienze dell'Atmosfera e del Clima, Consiglio Nazionale delle Ricerche, Lecce, Italy}

8 [3] {Istituto di Scienze dell'Atmosfera e del Clima, Consiglio Nazionale delle Ricerche, Rome, Italy}

9 [4] {Dipartimento di Scienze e Tecnologie Biologiche, Chimiche e Farmaceutiche (STEB-ICEF), Università di  
10 Palermo, Palermo, Italy}

11  
12 \*Corresponce to: F. Falcini (f.falcini@isac.cnr.it)

## 13 14 **Abstract**

15 Multidisciplinary studies are recently seeking to define diagnostic tools for fishery sustainability by  
16 coupling ichthyoplanktonic datasets, physical and bio-geochemical oceanographic measurements, and  
17 ocean modelling. The main goal of these efforts is the understanding of those processes that control  
18 fate and dispersion of fish larvae and eggs and thus tune the inter-annual variability of biomass of fish  
19 species. We here analyzed eggs and larvae distribution and biological features of *Sardinella aurita* in  
20 the northeast sector of the Sicily Channel (Mediterranean Sea) from ichthyoplanktonic data, collected  
21 during the 2010 and 2011 summer cruises. We also make use of satellite sea surface temperature, wind,  
22 and chlorophyll data to recognize the main oceanographic patterns that mark eggs and larvae transport  
23 processes, and we pair these data with Lagrangian runs. To provide a physical explanation of the  
24 transport processes that we observe, we hire-use a potential vorticity (PV) model that takes into account  
25 the role of wind stress in generating those cold filaments that are responsible for the offshore delivery  
26 of eggs and larvae. Our results show that the strong offshore transport towards Malta occurring in 2010  
27 is related to a persistent wind forcing along the southern Sicilian coast that generated an observable,  
28 high-PV cold filament. Such a pattern is not found in the 2011 analysis, which indeed shows an



29 | alongshore transport towards the recruiting area of Capo Passero and thus a more favorable condition  
30 | for sardinella larvae recruiting ~~with a weak offshore transport~~. Our results ~~want to~~ add some insights  
31 | regarding operational oceanography for sustainable fishery.

## 33 | 1 Introduction

34 | Small pelagic fish are essential elements of marine ecosystems due to their significant biomass at  
35 | intermediate levels of the food web, playing a considerable role in connecting the lower and upper  
36 | trophic levels (Rice, 1995; Bakun, 1996; Cury et al., 2000).

37 | The link among ocean currents, transport and distribution of small pelagic fish species, atmospheric  
38 | ~~forgeing~~forcing, and other environmental parameters is fundamental for the sustainable management of  
39 | fishery resources (Chavez et al., 2003; Pörtner and Knust, 2007). “Food” concentration and availability  
40 | is often modulated by oceanographic structures that have a crucial effect on the fate of several species,  
41 | especially during their larval and juvenile stages (McNamara and Houston, 1987; Cushing, 1990).  
42 | Moreover, dispersion and advection of fish larvae due to ocean fronts and filaments are the main causes  
43 | for the weakening of reproductive strategies. This is the case of the *Sardinella aurita* in the Sicily  
44 | Channel (Mediterranean Sea) and of similar small pelagic fishes such as the *Sardina pilchardus* and the  
45 | *Engraulis encrasicolus* (Olivar and Shelton, 1993; Lloret et al., 2000). Several studies have been  
46 | carried out to define the dynamics of transport of eggs and larvae and the effects on recruitments of  
47 | important commercial species in the Mediterranean sea, (i.e.; E. encrasicolus (Garcia et al 1996;  
48 | Agostini and Bakun, 2002; Lafuente et al., 2002; Cuttitta et. al., 2003, 2006; Somarakis and  
49 | Nikolioudakis, 2007; Sabates et al., 2007; Zarrad et.al, 2006; Sabates et al., 2013) and *S. pilchardus*  
50 | (Olivar et. al., 2001, 2003; Santos et. al., 2004; Alemany et.al., 2006; Tugores, 2011→)). Nevertheless,  
51 | knowledge on spatio-temporal distribution of eggs and larvae of *Sardinella aurita*, in relation to  
52 | mesoscale oceanographic and wind-forcing structures, are very limited in Mediterranean sea. In the  
53 | recent years an increasing abundance and gradual northward expansion of this specie has been reported  
54 | along different areas of the Mediterranean in correspondence to warming of the sea water (Sabatés et  
55 | al. 2006, Tsikliras and Antonopoulou, 2006, Sinovčić et al., 2004) with possible effects onf fisheries  
56 | catches.

57 | *Sardinella aurita* is a thermophilic pelagic fish that is widely distributed throughout the tropical and  
58 | subtropical seas of the world, including the entire Mediterranean and the Black Sea (Froese and Pauly,

59 2003). The reproductive period in the Mediterranean stretches over the warmest period of the year,  
60 from July to October (Palomera and Sabates, 1990; Somarakis et al., 2002; Tsikliras and  
61 Antonopoulou, 2006; Palomera et al., 2007) in accordance with its tropical origin (Ben Tuvia, 1960).  
62 Eggs and larvae of *Sardinella aurita* are often associated with warm coastal and ~~enriched-chlorophyll~~  
63 chlorophyll-enriched water (Ben Tuvia, 1960; Sabates et al., 2009). Affecting the dispersal mechanism,  
64 mesoscale oceanographic structure play a key role in shaping the spatial distribution of early life stages  
65 of this small pelagic species (Sabates 2009, 2013). However, studies about spawning area and  
66 advection of eggs and larvae in relation to a hydrographic condition along coasts of the northern part of  
67 the central Mediterranean Sea, are absent.

68 We here aim to “connect the dots” between *Sardinella aurita* eggs and larvae distribution, and the main  
69 oceanographic patterns that characterize ~~central Mediterranean Sea (i.e., the Sicily Channel (central~~  
70 Mediterranean Sea). ~~The This Sicily Channel channel~~ is mainly characterized by a meandering surface  
71 current, the Atlantic Ionian Stream (AIS), which transports the surface waters of Atlantic origin  
72 eastwards (Lermusiaux and Robinson, 1997). The climatological pattern of the AIS encircles two  
73 cyclonic vortices over the Adventure Bank and off Cape Passero, i.e., the Adventure Bank Vortex  
74 (ABV) and the Ionian Shelf Break Vortex (IBV), respectively, and it describes a pronounced  
75 anticyclonic meander in between, i.e., the Maltese Channel Crest (MCC). The most important feature  
76 for this study is, however, the role of wind (the Mistral in particular), which forms and enhances the  
77 coastal current flowing southeastward along Sicilian coast due to up-welling effects (Pratt and  
78 Whitehead, 2007; Falcini et al., 2015): blowing wind along the coastline creates offshore Ekman  
79 transport at the surface; consequently, water that are moved offshore are the replaced by deeper fluid  
80 that upwells and creates colder surface temperatures at the coast; the resultant sloping interface implies  
81 a cross-shelf pressure gradient that triggers a geostrophic, along-shore flow.

82 This wind-induced effect, moreover, This current often gives rise to the formation of  
83 cold filament that propagates offshore from the eastern Sicilian tip (i.e., Capo Passero; ~~Figure Fig. 1~~)  
84 (Bignami et al., 2008; ~~Faleini et al., 2015~~). These kind of jets are often related to instabilities formed at  
85 an upwelling front (Flament et al., 1985, Washburn and Armi, 1988, Wang et al., 1988, Strub et al.,  
86 1991 and Haynes et al., 1993), in particular, when a short-term wind bursts hit restricted areas of the  
87 near-shore sea surface (Bignami et al., 2008).

88

89 Palatella et al. (2014) introduced a Lagrangian approach (LaCasce, 2008) as a first step towards a better  
90 understanding of the relationship between anchovy population and sea surface dynamics. This type of  
91 study is focused, in particular, on the Lagrangian connectivity (Cowen et al., 2000) between spawning  
92 and nursery areas. More specifically, the approach seeks to estimate the amount of larvae coming from  
93 a certain spawning region that are able to reach a particular nursery region.

94 Here we focus on Lagrangian transport of *Sardinella aurita* eggs and larvae within the Sicily Channel  
95 during the summer spawnings of 2010 and 2011. By pairing this analysis with biological and  
96 environmental data we try to depict the dynamic connection between spawning and nursery areas and,  
97 in particular, the role of wind forcing in delivering *Sardinella aurita* larvae offshore. We finally ~~set and~~  
98 confirm some hypothesis regarding ~~the causes behind~~ the observed and simulated patterns by giving a  
99 physical interpretation of those Lagrangian dynamics (Falcini et al., 2015).

100

## 101 2 Data and Methods

### 102 2.1 The biological dataset

103 Ichthyoplanktonic data were collected during two cruises carried out from 25 June to 14 July 2010  
104 (Bansic 2010) and from 8 to 27 July 2011 (Bansic 2011) on board the R/V *Urania*, in correspondence  
105 with the main reproductive activity of this species (Whitehead, 1985). 190 and 131 station were  
106 sampled in Bansic 10 e Bansic 11, respectively (~~Figure Fig.~~ 1). Systematic sampling is constituted by a  
107 regular grid of stations ( $1/10^\circ \times 1/10^\circ$  along the continental shelf, and  $1/5^\circ \times 1/5^\circ$  ~~further~~ offshore)  
108 placed along transects perpendicular to the coast. Planktonic sampling was conducted using vertical  
109 CalVET (one mouth of 25 cm inlet diameter, 150  $\mu\text{m}$  mesh) and oblique Bongo 40 net (two mouth of  
110 40 cm inlet diameter, 200  $\mu\text{m}$  mesh, towed at 2 knots). The nets were hauled ~~from~~ within 5 m ~~from of~~  
111 the bottom to the surface, or from 100 m to the surface ~~at~~ deep stations. In each mouth, calibrated  
112 flow-meters were mounted ~~on~~ in order to calculate the volume of filtered water ( $\text{m}^3$ ). To preserve  
113 planktonic samples, borax-buffered solution of 4% formaldehyde and seawater (for CalVET and mouth  
114 1-Bongo 40 samples) and solution of 70% ethanol (for mouth 2-Bongo 40 samples) were used. In land  
115 based laboratory, all samples were observed ~~at binocular~~ under a microscope and fish eggs and larvae  
116 were sorted from the rest of the plankton. Eggs and larvae of *Sardinella aurita* were identified  
117 (Whitehead, 1988).

118 The number of fish eggs and larvae collected at each station was standardized to the number beneath a  
119 unit of sea surface ( $10 \text{ m}^2$ ) using the equation of Nonaka *et al.* (2000)  $Y_i = \frac{(10 \times d_i \times x_i)}{v_i}$ , where  $Y_i$  is  
120 the number of larvae/eggs of each species under  $10 \text{ m}^2$  of sea at station  $i$ ,  $x_i$  is the number of  
121 larvae/eggs taken at station  $i$ ,  $v_i$  is the volume of water filtered in  $\text{m}^3$  and  $d_i$  is the maximum depth  
122 reached by net.

123 Eggs and larvae preserved in formaldehyde were used for the determination of the stage of  
124 development. In particular, ~~eggs were assigned a stage staging of eggs were performed assigning~~  
125 number from 1 (stage after fecundation, with a single cell) to 11 (stage pre-hatching) following  
126 (Gamulin and Hure, 1955; Whitehead, 1988). We considered stage from 1 to 4 “early stage”, from 5 to  
127 8 “middle stage” and from 9 to 11 “late stage”.

128 Larvae were photographed through binocular stereo microscope with integrated camera and total length  
129 (TL, mm), ~~were obtained~~ from the analysis of image performed with suitably calibrated software  
130 (Image Pro Plus 6.0, Image Cybernetics, RoperIndistries, SilverSpring, MD, USA), ~~were obtained~~.  
131 Then, length classes ~~length~~ of 1 mm of magnitude were considered.

132

## 133 2.2 The remote sensing dataset

134 We pair the biological dataset with remote sensing data for (Table 1): sea surface temperature (SST),  
135 chlorophyll-a concentration (Chl). From these daily satellite data we evaluated cruise-averaged spatial  
136 maps (for each environmental parameter) that were superimposed to the entire ichthyoplanktonic data  
137 set, for both 2010 and 2011 datasets. This allowed to first recognize the main hydrographic features  
138 that occurred at Sicily Channel sea surface and the relations between Sardinella eggs and larvae  
139 distributions and environmental datasets.

140 We also analyze wind stress ( $\vec{\tau}$ ) and Ekman transport ( $\vec{m}$ ) from remote sensing. These quantities are  
141 derived from ocean surface 6-hourly wind data ( $\vec{U}_{wind}$ ), provided by the Cross-Calibrated Multi-  
142 Platform project (Table 1). Wind stress is obtained as

$$143 \quad \vec{\tau} = \rho_{air} C_d |\vec{U}_{wind}| \vec{U}_{wind}, \quad (1)$$

144 where  $\rho_{air}$  is the air density and the dimensionless friction coefficient  $C_d = 0.0012$  for  $0 < |\vec{U}_{wind}| < 11$   
 145  $\text{m s}^{-1}$  and  $C_d = 0.00049$  for  $|\vec{U}_{wind}| \geq 11 \text{ m s}^{-1}$  (Large and Pond, 1981; McClain and Firestone, 1993).  
 146 Ekman transport is then calculated as (Pickett and Paduan, 2003)

$$147 \quad \vec{M} = (\rho_{water} f)^{-1} \vec{\tau} \times \hat{k}, \quad (2)$$

148 where  $\rho_{water}$  is the water density,  $f$  the Coriolis parameter, and  $\hat{k}$  is the vertical unit vector.

149

## 150 2.3 The Lagrangian simulations

151 Modern Lagrangian modelling techniques have been developed recently to simulate tracer trajectories  
 152 ~~advected by from Eulerian velocity fields~~ marine currents ~~from available velocity fields.~~, such as those  
 153 ~~provided by the Mediterranean Forecasting System (MFS) (Tonani et al., 2008). The main model w~~We  
 154 ~~here have used the model is~~ provided by the Mediterranean Forecasting System (MFS; see, e.g., Tonani  
 155 et al., 2008, ~~for a detailed description of the Ocean model~~) as Eulerian input. ~~The~~ Its domain covers all  
 156 the Mediterranean basin; ~~the Horizontal~~ horizontal ~~and vertical spatial resolution are, respectively, is~~  
 157 1/16 x 1/16 degree (~ 6.5 km) ~~and;~~ the model has 72 vertical layers, ranging from 1.5 m to 5000 m  
 158 depth; wind forcing is provided by ECMWF data every six hours. ~~The~~ Daily ~~daily~~ re-analysis velocity  
 159 fields from the MFS model ~~are~~ used for the large-scale circulation while a 2D kinematic eddy field and  
 160 a 3D convective cell field are added to the main model in order to ~~to~~ compensate the lack of,  
 161 ~~respectively,~~ effective mesoscale turbulent dispersion and vertical mixing in the mixed layer, as  
 162 discussed below (Lacorata et al., 2008, 2014; Palatella et al., 2014). The boundary conditions are open  
 163 (relatively to the Sicily Channel sub-domain), with rebound conditions of the Lagrangian particles  
 164 against the coasts (an accurate modelling of the circulation in proximity of coastal boundaries is outside  
 165 the capabilities of the Ocean model ~~we have used~~). ~~Wind forcing is provided by ECMWF data every~~  
 166 ~~six hours.~~ The period covered by the simulation goes from June, 1<sup>st</sup> to September, 30<sup>th</sup>, for both 2010  
 167 and 2011. We assumed a source of passive neutrally buoyant particles emitting at constant rate in the  
 168 period from June, 1<sup>st</sup> to September, 15<sup>th</sup>. The total number of numerical trajectories analyzed in each  
 169 run is 25600.

170 As mentioned above ~~Broadly speaking~~, there are two main issues related to the simulation of transport  
171 and mixing of particles ~~in from~~ an ocean circulation model: (i) the lack of resolution of meso- and  
172 submeso-scale horizontal motions and (ii) the underestimation of the vertical mixing in the upper layer.  
173 In our Lagrangian approach ~~both these two instances aspects drawbacks~~ are treated by adopting a  
174 kinematic Lagrangian modelling strategy. ~~Conservative Deterministic deterministic~~ chaotic flows are  
175 exploited to work very efficiently at this scope, since they can generate trajectories that accurately  
176 simulate (at least at a low order moment level in terms of statistics) the typical small-scale turbulent  
177 motions affecting, which in turn affect the dispersion of a given tracer distribution at early stage  
178 (Lacorata et al., 2008, 2014; Palatella et al., 2014). At this scope ~~In order to capture such a dispersion~~  
179 the kinematic velocity fields are ~~is~~ composed by 2D or 3D time oscillating convective cells of various  
180 length sizes and with a given spatio-temporal scaling relationship (e.g. Kolmogorov's scaling).  
181 Anomalous behaviors due to unrealistic ~~the~~ “sweeping effect”, i.e., a known drawback affecting  
182 kinematic simulations of turbulence, are ruled out by adopting the quasi-Lagrangian coordinates  
183 technique (Lacorata et al, 2008). ~~Such a pioneering approach represents a novelty, since it uses a~~  
184 kinematic model for mesoscale turbulent dispersion as coupled to a large-scale ocean circulation model  
185 (see ~~D~~details about on the the kinematic model set up of the kinematic models, the 3D vertical mixing  
186 model, and the 2D mesoscale turbulence model are the same as in Palatella et al., 2014, for the 3D  
187 vertical mixing model, and as in and Lacorata et al., 2014, for the) 2D mesoscale turbulence model.

188

## 189 **3 Results**

### 190 **3.1 Spatial distribution pattern of eggs and larvae**

191 Spatial analysis of early life stages of *Sardinella aurita* showed a very patchy distribution among  
192 sampling stations. As other small pelagic fish, this discontinuous pattern typically reflects the spawning  
193 behaviour of adults, characterized by brief spawning events in a localized point of the study area.

194 From Ichthyoplanktonic data ~~have revealed we found that~~ the main ~~principal~~ spawning and retention  
195 areas of for the *Sardinella aurita*, on the Italian side of the Sicily Channel (Figures 1). This the south-  
196 eastern part of the Sicilian coastal zone, i.e. off Capo Passero, ~~has been identified as the main~~  
197 spawning area for this species (Figure-Fig. 1). Indeed, this area exhibited the highest value of density of  
198 eggs for both years. However, we also found different spatio-temporal patterns of abundance and  
199 distribution of eggs and larvae. In 2010 the overall density of eggs and larvae was greater than ~~higher~~

200 ~~with respect to~~ in the 2011 (mean of 36.65 against 14.13 eggs/10m<sup>2</sup> in survey 2010 and 2011; mean of  
201 22.83 against 9.38 larvae/10m<sup>2</sup> in survey 2010 and 2011). Malta zone showed the largest fluctuations  
202 of abundance between the two years~~The main abundance differences between 2010 and 2011 in Malta~~  
203 ~~zone~~ (Figure-Fig. 1). Eggs and larvae were found also in the northwestern part of the study area, the  
204 Adventure bank, although in very low abundance in both years (Figure-Fig. 1).

205 Analysis of egg stages revealed different spatial distributions~~Analysis of staging of eggs revealed a~~  
206 ~~different spatial distribution~~ of stage in the south-eastern part of the Sicily Channel. In 2010, the areas  
207 off Capo Passero was characterized by the presence of all different egg stages in with similar amounts  
208 concentrations (early stage: 36%; middle stage: 38%; late stage: 26%) ~~Otherwise, in while, in the~~  
209 region off Malta, we observed a predominance of middle and late stage (i.e., early stage: 20%; middle  
210 stage: 53%; late stage: 27%). ~~Differently~~On the other hand, in 2011 we observed a dominance of late  
211 stage eggs off Capo Passero (early stage: 7%; middle stage: 31%; late stage: 62%). For this year, ~~we~~  
212 ~~also recognize that~~ *Sardinella aurita* eggs ~~are were~~exclusively found only off Capo Passero, with  
213 exception of one eggs of stage 6 (middle stage) on Adventure Bank; no eggs were therefore found off  
214 Malta, and a dominance of late stages was emerged.

215 Spatial distribution of the length classes of larvae (total length ranging from 2 to 12 mm) are shown in  
216 Figure 2. In 2010 the zone off Capo Passero was characterized by a dimensional-length range of 3 - 9  
217 mm while, in the zone off Malta, we observed larvae ~~longer than 8 mm that range from (range 2 to 12~~  
218 ~~mm)~~. ~~This indicates that Sardinella aurita larvae did not find the ideal dynamic conditions for a local~~  
219 ~~recruiting and were likely delivered offshore~~. The 2011 showed a ~~more~~ different pattern: off Capo  
220 Passero we observe larvae that belong to a wide dimensional-length range (from 2 to 11 mm) while,  
221 around Malta, we ~~recorded very few larvae did not record any larvae~~.

222 These evidences set some hypotheses regarding~~mark a the~~ joint action ~~of between~~ *in situ* spawning  
223 ~~(early stage)~~ and eggs/larvae advection due to mesoscale, coastal oceanographic structures. In 2010, the  
224 presence of i) several stages of Sardinella aurita eggs off Capo Passero; ii) middle to late stages off  
225 Malta; and a-iii) small lengthless dimensional range of larvae ~~in the southeast coast of Sicily off Capo~~  
226 Passero; and iv) a larger range off Malta ~~could be the mutual effect of~~ suggest an offshore advection of  
227 eggs and larvae from Capo Passero to Malta, reasonably due to wind-induced effects. Such a  
228 mechanism seems not to be active in 2011. Conversely, these results should be explained by the lack of  
229 durable oceanographic structures able to remove early life stages of Sardinella aurita from the

230 spawning area (i.e., off Capo Passero), a counter hypothesis that might not be realistic in such a  
231 dynamic region. We therefore pursue the idea that the offshore transport occurring in 2010 likely  
232 delivered *Sardinella aurita* larvae far from the ideal recruiting area of Capo Passero.

233 Finally we point out that, for both years, the wide distribution of egg stages off Capo Passero also  
234 suggests that this location - in addition to its in situ spawning eggs - receives eggs that are released all  
235 along the Sicilian coast and transported by coastal currents (Agostini and Bakun, 2002; Cuttitta et al.,  
236 2006; Falcini et al., 2015).

### 238 3.2 Results from Lagrangian Simulations

239 The hypothesis of a more intense offshore transport of *Sardinella aurita* occurred from the recruiting  
240 area of Capo Passero during the summer 2010 with respect to the 2011 is here explored by means of  
241 Lagrangian runs (~~Figure-Fig. 3;- and in Supplementary Information~~). These simulations confirm the  
242 presence of a narrow filament that dynamically connects the spawning/recruiting area off Capo Passero  
243 with Malta. During the middle of June 2010 we notice a strong southward advection of particles that  
244 are thus delivered to eastern sector of Malta in a few days (i.e., ~ 50 km in 5 days that corresponds to a  
245 surface current of ~10 cm/s) by a particular branch of the Lagrangian trajectories. In particular, we  
246 observe two events with this intensity: one around ~~the June 10<sup>th</sup> of June~~ and the second inat between  
247 ~~the June 30<sup>th</sup> of June~~ and ~~the July 8<sup>th</sup> of July~~. The 2011 shows a similar pattern, although there is no  
248 evidence of a Lagrangian preferential path that connects Capo Passero to the eastern side of Malta and,  
249 for the whole July, the southward advection is much weaker with respect to the 2010 case. The  
250 comparison between these two scenarios is further stressed by the MFS Eulerian velocity fields (Tonani  
251 et al., 2008), averaged through the two oceanographic surveys (~~Figure-Fig. 4~~). The 2011 shows a much  
252 weaker velocity field – and the absence of the cold filament – that did not deliver larvae offshore.

### 254 3.3 Results from the satellite datasets

255 SST and Chl concentration satellite patterns confirm the hypothesis of two different oceanographic  
256 conditions in the two study years (~~Figure-Fig. 5~~). In the 2010 the Sicily Channel was characterized by a  
257 colder surface water and a higher Chl concentration (mean SST=23.59°C; mean Chl= 0.044 µg/l) with



258 compared to the 2011 (mean SST=25.08; mean Chl = 0.042  $\mu\text{g/l}$ ). In particular, in 2010 maps  
259 evidenced a cold and Chl-rich structure that protrudes offshore from the Capo Passero (~~Figure-Fig.~~  
260 ~~6A6a, Bb~~). Such a structure is characterized by a SST  $\approx 23.20^\circ\text{C}$  and a Chl  $\approx 0.07 \mu\text{g/l}$ , and traces a  
261 curved path (i.e., a filament). The 2011 does not show a similar pattern.

262 In seeking to understand the role of upwelling in the formation of such a cold ~~and~~, Chl-rich filament,  
263 we find a comforting agreement from wind stress and Ekman transport maps (Supplementary  
264 ~~Information~~). Between the 30<sup>th</sup> of June and the 8<sup>th</sup> of July 2010 a significant Ekman transport likely  
265 induced the formation of an upwelling induced coastal current (~~Figure-Fig.~~ 6). Although the 2011 is  
266 also characterized by strong wind events, it does not record the same persistency that we observe in  
267 ~~2010, when the Mistral wind blew steadily for the 2010, where the Mistral wind steadily blown for 8~~  
268 ~~days (see in the Supplementary Information). The different wind pattern that we observe for the two~~  
269 ~~years is better investigated in the next section.~~

270

#### 271 4 The surface cold filament model

272 Based on our results, we reasonably hypothesize that the particularly strong Mistral wind pattern, and  
273 thus ~~front instabilities related to the offshore the coastal Ekman transport layer~~ occurred during the  
274 ~~summer spawning in 2010~~, triggered the southward transport of *Sardinella aurita* larvae and eggs ~~along~~  
275 ~~the from~~ Capo Passero, ~~along the and~~ chlorophyll reach filament. To diagnose this pattern, and to  
276 provide a mechanistic explanation regarding the link between the wind field and the onset of the cross-  
277 shore transport, we ~~use a surface cold filament model hire the surface cold filament model~~ (Bignami et  
278 al., 2008). Wind forcing can directly produces shelf-blocked jets that are subsequently driven offshore  
279 by the general circulation (Crépon and Richez, 1982; McCreary et al., 1989; Salusti, 1998). The model  
280 describes the ~~origin potential of to~~ these cold filaments and jets ~~to propagate offshore and to maintain~~  
281 ~~their coherent structure based on their potential vorticity (PV). These jets, indeed, are~~ generated by a  
282 strong PV input ~~of potential vorticity (PV) into the sea~~ due to upwelling and/or the funneling of strong,  
283 cold, and short-term wind bursts that blow over a restricted, shallow area of the sea surface near the  
284 coast (Holland, 1967). This PV ( $\Pi$ ) increase, due to the wind stress ( $\vec{\tau}$ ), is described by

$$285 \frac{d\Pi}{dt} = \frac{1}{\rho h} (\nabla \times \vec{\tau})_z, \quad (3)$$

286 where  $\rho$  is the water density,  $h$  is the cold water thickness, and the subscript  $z$  indicates the third  
287 component (i.e., the vertical one) of the curl.

288 Equation (34) can be integrated in order to estimate, and to compare, the amount of PV accumulated on  
289 the shelf area during the two summer spawning periods in 2010 and 2011:

$$290 \quad \Pi = \frac{1}{\rho h} \int_0^t \left( \frac{\partial \tau_y}{\partial x} - \frac{\partial \tau_x}{\partial y} \right) dt \quad (4)$$

291 Figure 7 shows the temporal integral of the curl of wind stress in Eq. (4) and fully confirms our  
292 hypothesis. Based on the surface cold filament model, the higher PV- (i.e., higher  $(\nabla \times \vec{\tau})_z$ ) we observe  
293 in ~~the~~ 2010 – with respect to the 2011 – marks the strong role of the wind stress in “loading” PV to the  
294 ~~the~~ coastal water-PV. Once the high PV is set such a strong and localized input does not remain  
295 confined to the coastal zone, but propagates offshore as a filaments ~~or jets~~ (Bignami et al., 2008).

296 We therefore point out that Ekman transport due to Mistral wind was particularly active for both years  
297 (Supplementary Information), thus generating a cold coastal current that efficiently transported eggs  
298 and larvae to Capo Passero from the whole Sicilian coast. However, only the 2010 case was  
299 characterized by a high PV input able to trigger the filament that delivered eggs and larvae offshore  
300 (i.e., around Malta).

301

## 302 5 Discussions and Conclusions

303 The dynamics of marine surface layer plays a fundamental, and for many aspects unpredictable, role as  
304 far as the life and the evolution of pelagic species are concerned. In the early stage, fish larvae move as  
305 passively advected by the currents, and their fate is strictly related to their Lagrangian pathways across  
306 the sea and to the selection rules that may strongly affect their population. A systematic study of the  
307 dynamical evolution of marine species can only be assessed by means of accurate modeling of velocity  
308 fields and Lagrangian transport, as well as by a deep understanding of the physical processes that rule  
309 larvae fate and dispersion.

310 Our work provide some insights regarding the potential of remote sensing and Lagrangian techniques  
311 to monitor and predict the abundance of small pelagic larvae in recruiting areas. Cross-shore transport  
312 phenomena remove small pelagic eggs and larvae from the main, coastal conveyor belt that would

313 deliver them to the recruiting areas (Garcia-Lafuente et al., 2002; Falcini et al., 2015). Estimating the  
314 rate of this removal is at the base of the prediction of the subsequent biomass, especially for short  
315 living species.

316 Our multidisciplinary analysis, by comparing two summer spawning season in 2010 and 2011, shows  
317 that intense wind-induced phenomena (i.e., PV inputs due to wind bursts blowing over shallow, coastal  
318 areas) lead to cross-shore transport of *Sardinella aurita* larvae from the spawning/recruiting area of  
319 Capo Passero to Malta. This is the case of 2010, where we observed from the ichthyoplanktonic dataset  
320 a large larvae concentration off Malta, also marked by a wide dimensional-length range. The pairing of  
321 Lagrangian runs and the analysis of environmental parameters measured from remote sensing (i.e.,  
322 SST, Chl, and wind stress) confirms, for this hereyear, the presence of a cold, chlorophyll-rich filament  
323 that delivered the larvae to Malta from the Sicilian coast.

324 To give a mechanistic explanation to these correlations and to provide a diagnostic tool for the  
325 understanding of the role of Mistral wind in such a dynamics we make use of a PV theory for the  
326 evolution of surface cold filaments. Our application demonstrates that PV in 2010, relative to 2011  
327 higher PV occurred in the 2010, with respect to the 2011, was responsible for the formation a cross-  
328 shore jet.

329 The expected benefits for fisheries management in strategic areas, in the Mediterranean, as well as in  
330 other ocean basins, will consist in having a major and more detailed information about preferential  
331 sources and recruitment areas, in order to better estimate and possibly regulate the amount of future  
332 biomass. Our findings can indeed be easily applied to those geographical regions where fate and  
333 distribution of small pelagic larvae are potentially affected by wind effects (e.g., Gulf of Tunis,  
334 northeast Spanish coast, the northern Aegean Sea, and California Current System). We believe that our  
335 approach, paired with the use of operational oceanographic tools, can lead to very interesting and  
336 useful results for a sustainable fishery management.

337

### 338 **Acknowledgements**

339 We thank Prof. M. Kurgansky, Dr. E. Salusti, and Dr. J. Kozarek for insightful discussions at the initial  
340 stage of our study. We also thank Dr. A. Lanotte for her technical and scientific help regarding the  
341 Lagrangian simulations. We are grateful to all those who provided the publicly available ocean data

342 that made this work possible. This work has been funded supported by the SSD PESCA and the  
343 RITMARE Italian Research Ministry (MIUR) Projects.

344

## 345 **Figure Captions**

346 **Figure 1.** Map of the study area (i.e., Sicily Channel) showing the sampling stations. Bathymetry is  
347 indicated by contours~~are indicated contours~~ and by background colors, from cyan (shallower) to blue  
348 (deeper). The isobaths of 100, 200 and 1000 m are shown. Red circles and yellow squares represent  
349 larval (upper panels) and eggs (~~down~~lower panels) density of *Sardinella aurita* during 2010 (left) and  
350 2011(right) surveys, respectively. The main points of interest are indicated (i.e., Adventure Bank,  
351 Malta, and Capo Passero).

352 **Figure 2.** Frequency histograms of the total lengths (TLs) measured off Adventure Bank, Capo  
353 Passero, and Malta during the two Bansic 2010 and 2011 cruises.

354 **Figure 3.** Lagrangian run snapshot on 8 July 2010 showing the net transport of *Sardinella Aurita* larvae  
355 (red dots) from Capo Passero to Malta that occurs along the cold filament forming off Capo Passero.

356 **Figure 4.** Cruise averaged Eulerian velocity fields for the two Bansic 2010 and 2011 cruises: 25 June  
357 to 14 July 2010 and 8 to 27 July 2011, respectively.

358 **Figure 5.** Cruise averaged Sea Surface Temperature (aA, cC) and Chlorophyll concentration (bB, dD)  
359 for the two Bansic 2010 and 2011 cruises.

360 **Figure 6.** Daily Ekman transport during the Bansic 2010 cruise, from 29 June to 10 July.

361 **Figure 7.** Integral of the curl of wind stress  $\rho h \Pi$  (Ns/m<sup>3</sup>) (see Eq. 4) performed throughout the Bansic  
362 2010 (25 June to 14 July) and Bansic 2011 (8 to 27 July) cruises showing the more intense potential  
363 vorticity increase that occurred in 2010. Such a potential vorticity input led to the formation-offshore  
364 propagation of the cold filament.

365

## 366 **Supplementary Information**

367 **S1.** Maps of daily wind stress for the Bansic 2010 cruise

368 **S2.** Maps of daily wind stress for the Bansic 2011 cruise

- 369 **S3.** Maps of daily Ekman transport for the Bansic 2010 cruise
- 370 **S4.** Maps of daily Ekman transport for the Bansic 2011 cruise
- 371 **S5.** Animated gif showing the Lagrangian transport of *Sardinella Aurita* during the Bansic 2010 cruise.
- 372 **S6.** Animated gif showing the Lagrangian transport of *Sardinella Aurita* during the Bansic 2011 ~~0~~  
373 cruise.

374

## 375 **References**

- 376 Agostini, V. N. and Bakun, A.: Ocean triads' in the Mediterranean Sea: physical mechanisms  
377 potentially structuring reproductive habitat suitability (with example application to European anchovy,  
378 *Engraulis encrasicolus*). Fish. Oceanogr., 11(3), 129-142, 2002.
- 379 Alemany, F., Álvarez, I., García, A., Cortés, D., Ramírez, T., Quintanilla, J., ... and Rodríguez, J. M.:  
380 Postflexion larvae and juvenile daily growth patterns of the Alborán Sea sardine (*Sardina pilchardus*  
381 Walb.): influence of wind. Sci. Mar., 70(S2), 93-104, 2006.
- 382 Bakun, A.: Patterns in the Ocean. Ocean Processes and Marine Population Dynamics. California Dea  
383 Grant College System, C.A., 1996.
- 384 Ben-Tuvia, A.: Synopsis of biological data on *Sardinella aurita* of the Mediterranean Sea and other  
385 waters. Fisheries Division, Biology Branch, Food and Agriculture Organization of the United Nations,  
386 1960.
- 387 Bignami, F., Böhm, E., D'Acunzo, E., D'Archino, R., and Salusti, E.: On the dynamics of surface cold  
388 filaments in the Mediterranean Sea, J. Marine Syst., 74(1), 429-442, 2008.
- 389 Chavez F. P., Ryan J., Lluch-Cota S. E., and Niquen M.: From Anchovies to Sardines and Back:  
390 Multidecadal Change in the Pacific Ocean, Science, 299, 217-221, 2006.
- 391 Cowen, R. K., Lwiza, K. M. M., Sponaugle, S., Paris, C. B., and Olson, D. B.: Connectivity of marine  
392 populations: Open or closed?, Science, 287, 857–859, 2000.
- 393 Crépon, M. and Richez, C.: Transient upwelling generated by two dimensional forcing and variability  
394 in the coastline, J. Phys. Oceanogr. 12, 1437–1457, 1982.

- 395 Cury, P., Bakun, A., Crawford, R. J. M., Jarre, A., Quinones, R.A., Shannon, L. J. H., and Verheye, M.:  
396 Small pelagic in upwelling systems: patterns of interaction and structural changes in “wasp-waist”  
397 ecosystems, *ICES J. Mar. Sci.*, 57, 603–618, 2000.
- 398 Cushing, D. H.: Plankton production and year-class strength in fish populations: an update of the  
399 match/mismatch hypothesis, *Adv. Mar. Biol.*, 26, 249-293, 1990.
- 400 Cuttitta, A., Carini, V., Patti, B., Bonanno, A., Basilone, G., Mazzola, S., ... and Cavalcante, C.:  
401 Anchovy egg and larval distribution in relation to biological and physical oceanography in the Strait of  
402 Sicily. In *Migrations and Dispersal of Marine Organisms*, Springer Netherlands, 2003.
- 403 Cuttitta, A., Guisande, C., Riveiro, I., Maneiro, I., Patti, B., Vergara, A. R., ... and Mazzola, S.: Factors  
404 structuring reproductive habitat suitability of *Engraulis encrasicolus* in the south coast of Sicily, *J. Fish.*  
405 *Biol.*, 68(1), 264-275, 2006.
- 406 Falcini, F., Palatella, L., Cuttitta, A., Nardelli, B. B., Lacorata, G., Lanotte, A. S., ... and Santoleri, R.:  
407 The Role of Hydrodynamic Processes on Anchovy Eggs and Larvae Distribution in the Sicily Channel  
408 (Mediterranean Sea): A Case Study for the 2004 Data Set, *PloS One*, 10(4), 2015.
- 409 [Flament, P., Armi, L., & Washburn, L.: The evolving structure of an upwelling filament. \*Journal of\*](#)  
410 [\*Geophysical Research: Oceans\* \(1978–2012\), 90\(C6\), 11765-11778, 1985.](#)
- 411 Froese, R. and Pauly, D. (eds.): FishBase, World Wide Web electronic publication, [www.fishbase.org](http://www.fishbase.org),  
412 2003.
- 413 Gamulin, T. and Hure, J.: Contribution a la connaissance de l’ecologie de la ponte de la sardine  
414 (*Sardina pilchardus* Walb.) dans l’Adriatique. *Acta Adriatica*, 7, 1– 23, 1955.
- 415 Garcia, A. and Palomera, I.: Anchovy early life history and its relation to its surrounding environment  
416 in the Western Mediterranean basin, *Sci. Mar.*, 60(S2), 155–166. 1996.
- 417 [Haynes, E., Barton, D., Pilling, I.: Development, persistence, and variability of upwelling filaments off](#)  
418 [the Atlantic coast of the Iberian Peninsula, \*J. Geophys. Res.\* 98 \(C12\), 22681–22692, 1993.](#)
- 419 Holland, W.R.: On the wind-driven circulation in an ocean with bottom topography, *Tellus*, 19, 582–  
420 600, 1967.
- 421 LaCasce, J. H.: Statistics from Lagrangian observations, *Prog. Oceanogr.*, 77(1), 1-29, 2008.

422 Lacorata, G., Mazzino, A., and Rizza, U.: A 3D chaotic model for subgrid turbulent dispersion in large-  
423 eddy simulations, *J. Atmos. Sci.*, 65, 2389–2401, 2008.

424 Lafuente, J. G., García, A., Mazzola, S., Quintanilla, L., Delgado, J., Cuttita, A., and Patti, B.:  
425 Hydrographic phenomena influencing early life stages of the Sicilian Channel anchovy, *Fish.*  
426 *Oceanogr.*, 11(1), 31-44, 2002.

427 Large, W. G. and Pond S.: Open ocean momentum flux measurements in moderate to strong winds, *J*  
428 *Phys. Oceanogr.*, 11, 324-336, 1981.

429 Lermusiaux, P. F. J. and Robinson A. R.: Features of dominant mesoscale variability, circulation  
430 patterns and dynamics in the Strait of Sicily, *Deep Sea Res. Part I*, 48, 1953–1997, 2001.

431 Lloret, J., Lleó, J., and Solé, I.: Time series modelling of landings in Northwest Mediterranean Sea,  
432 *ICES J. Mar. Sci.*, 57, 171-184, 2000.

433 McClain, C. R. and Firestone, J.: An investigation of Ekman upwelling in the North Atlantic, *J.*  
434 *Geophys. Res. Oceans*, 98, 12327-12339, 1993.

435 McCreary, J. P., Lee, H. S., and Enfield, D. B.: The response of the coastal ocean to strong offshore  
436 winds: With application to circulations in the Gulfs of Tehuantepec and Papagayo, *J. Mar. Res.*, 47(1),  
437 81-109, 1989.

438 McNamara, J.M. and Houston, A.I.: Starvation and predation as factors limiting population size,  
439 *Ecology*, 68, 1515–1519, 1987

440 Nonaka, M., Fushimi, H., and Yamakawa, T.: The spiny lobster fishery in Japan and restocking, *Spiny*  
441 *Lobsters Fisheries and Culture*, 221-242, 2000.

442 Olivar, M. P., Shelton, P. A.: Larval fish assemblages of the Benguela Current, *B. Mar. Sci.*, 53, 450-  
443 474, 1993.

444 Olivar, M.P., Salat, J., and Palomera, I.: A comparative study of spatial distribution patterns of the  
445 early stages of anchovy and pilchard in the NW Mediterranean Sea, *Mar. Ecol-Prog. Ser.*, 217, 111–  
446 120, 2001.

447 Olivar, M.P., Catalan, I.A., Emelianov, M., Fernandez de Puelles, M.L.: Early stages of *Sardina*  
448 *pilchardus* and environmental anomalies in the North Western Mediterranean, *Estuar. Coast. Shelf S.*,  
449 56, 609–619, 2003.

450 Palatella, L., Bignami, F., Falcini, F., Lacorata, G., Lanotte, A. S., and Santoleri, R.: Lagrangian  
451 simulations and interannual variability of anchovy egg and larva dispersal in the Sicily Channel, *J.*  
452 *Geophys. Res.: Oceans*, 119(2), 1306-1323, 2014.

453 Palomera, I. and Sabates, A.: Co-occurrence of *Engraulis encrasicolus* and *Sardinella aurita* eggs and  
454 larvae in the western Mediterranean, *Sci. Mar.*, 54, 51–67, 1990.

455 Palomera, I., Olivar, M. P., Salat, J., Sabatés, A., Coll, M., García, A., and Morales-Nin, B.: Small  
456 pelagic fish in the NW Mediterranean Sea: an ecological review. *Progr. Oceanogr.*, 74(2), 377-396,  
457 2007.

458 Pickett, M. H. and Paduan, J. D.: Ekman transport and pumping in the California Current based on the  
459 US Navy's high-resolution atmospheric model (COAMPS), *J. Geophys. Res. Oceans*, 108(C10), 2003.

460 Pisano, A., Buongiorno Nardelli, B., Rinaldi, E., Tronconi, C., and Santoleri, R.: The New  
461 Mediterranean Optimally Interpolated Pathfinder AVHRR SST Dataset (1982 - 2012): Validation and  
462 Time Series Analysis. Under Review in *Remote Sens. Environ.*, 2015.

463 Pörtner, H.O. and Knust, R.: Climate change affects marine fishes through the oxygen limitation of  
464 thermal tolerance, *Science*, 315, 95-97, 2007.

465 Pratt, L. L. and Whitehead, J. A.: Rotating hydraulics: nonlinear topographic effects in the ocean and  
466 atmosphere (Vol. 36). Springer, 2007.

467 Rice, J.: Food web theory, marine food webs and what climate changes may do to northern marine fish  
468 populations. In: Beamish, R.J. (Ed.), *Climate Change and Northern Fish Populations*. Canadian Special  
469 Publication Fish Aquatic Science, 121, 561–568, 1995

470 Sabatés, A., Salat, J., Palomera, I., Emelianov, M., Fernández de Puelles, M. L., and Olivar, M. P.:  
471 Advection of anchovy (*Engraulis encrasicolus*) larvae along the Catalan continental slope (NW  
472 Mediterranean), *Fish. Oceanogr.*, 16(2), 130-141, 2007.



- 473 Sabatés, A., Salat, J., Raya, V., Emelianov, M., and Segura i Noguera, M. D. M.: Spawning  
474 environmental conditions of *Sardinella aurita* at the northern limit of its distribution range, the western  
475 Mediterranean, *Mar. Ecol-Prog. Ser.*, 385, 227-236, 2009.
- 476 Sabatés, A., Salat, J., Raya, V., and Emelianov, M.: Role of mesoscale eddies in shaping the spatial  
477 distribution of the coexisting *Engraulis encrasicolus* and *Sardinella aurita* larvae in the northwestern  
478 Mediterranean, *J. Marine Syst.*, 111, 108-119, 2013.
- 479 Salusti, E.: Satellite images of upwellings and cold filament dynamics as transient effects of violent  
480 air-sea interactions downstream from the island of Sardinia (western Mediterranean Sea). *J. Geophys.*  
481 *Res. Oceans (1978–2012)*, 103(C2), 3013-3031, 1998.
- 482 Santos, A. M. P., Peliz, A., Dubert, J., Oliveira, P. B., Angélico, M. M., and Ré, P.: Impact of a winter  
483 upwelling event on the distribution and transport of sardine (*Sardina pilchardus*) eggs and larvae off  
484 western Iberia: a retention mechanism, *Cont. Shelf Res.*, 24(2), 149-165, 2004.
- 485 Sinovčić, G., Franičević, M., and Čikeš Keč, V.: Unusual occurrence and some aspects of biology of  
486 juvenile gilt sardine (*Sardinella aurita* Valenciennes, 1847) in the Zrmanja River estuary (eastern  
487 Adriatic), *J. Appl. Ichthyol.*, 20(1), 53-57, 2004.
- 488 Somarakis, S., Drakopoulos, P., and Filippou, V.: Distribution and abundance of larval fish in the  
489 northern Aegean Sea—eastern Mediterranean—in relation to early summer oceanographic conditions,  
490 *J. Plankton Res.*, 24(4), 339-358, 2002.
- 491 Somarakis, S. and Nikolioudakis, N.: Oceanographic habitat, growth and mortality of larval anchovy  
492 (*Engraulis encrasicolus*) in the northern Aegean Sea (eastern Mediterranean), *Mar. Biol.*, 152(5), 1143-  
493 1158, 2007.
- 494 [Strub, P. T., Kosro, P. M., & Huyer, A.: The nature of the cold filaments in the California Current](#)  
495 [System. \*Journal of Geophysical Research: Oceans \(1978–2012\)\*, 96\(C8\), 14743-14768, 1991.](#)
- 496 Tonani, M., Pinardi, N., Dobricic, S., Pujol I., and Fratianni C.: A high-resolution free-surface model of  
497 the Mediterranean Sea. *Ocean Sci.*, 4, 1–14, 2008.
- 498 Tsikliras, A. C. and Antonopoulou, E.: Reproductive biology of round sardinella (*Sardinella aurita*) in  
499 north-eastern Mediterranean, *Sci. Mar.*, 70(2), 281-290, 2006.

500 Tugores, M. P., Giannoulaki, M., Iglesias, M., Bonanno, A., Ticina, V., Leonori, I., ... and Valavanis,  
501 V.: Habitat suitability modelling for sardine *Sardina pilchardus* in a highly diverse ecosystem: the  
502 Mediterranean Sea, *Mar. Ecol-Prog. Ser.*, 443, 181-205, 2011.

503 Volpe, G., Santoleri, R., Vellucci, V., Ribera d Acalà, M., Marullo, S., and D'Ortenzio, F.: The colour  
504 of the Mediterranean Sea: Global versus regional bio-optical algorithms evaluation and implication for  
505 satellite chlorophyll estimates, *Remote Sens. Environ.*, 107, 625-638, 2007.

506 [Wang, D. P., Vieira, M. E., Salat, J., Tintore, J., & La Violette, P. E.: A shelf/slope frontal filament off](#)  
507 [the northeast Spanish coast. \*Journal of Marine Research\*, 46\(2\), 321-332, 1988.](#)

508 [Washburn, L., & Armi, L.: Observations of frontal instabilities on an upwelling filament. \*Journal of\*](#)  
509 [physical oceanography, 18\(8\), 1075-1092, 1988.](#)

510 Whitehead, P. J. P., Nelson, G. J., and Wongratana, T.: Clupeoid fishes of the world (suborder  
511 Clupeioidi). Rome: United Nations Development Programme, ISBN 92-5-102667-X, 1988.

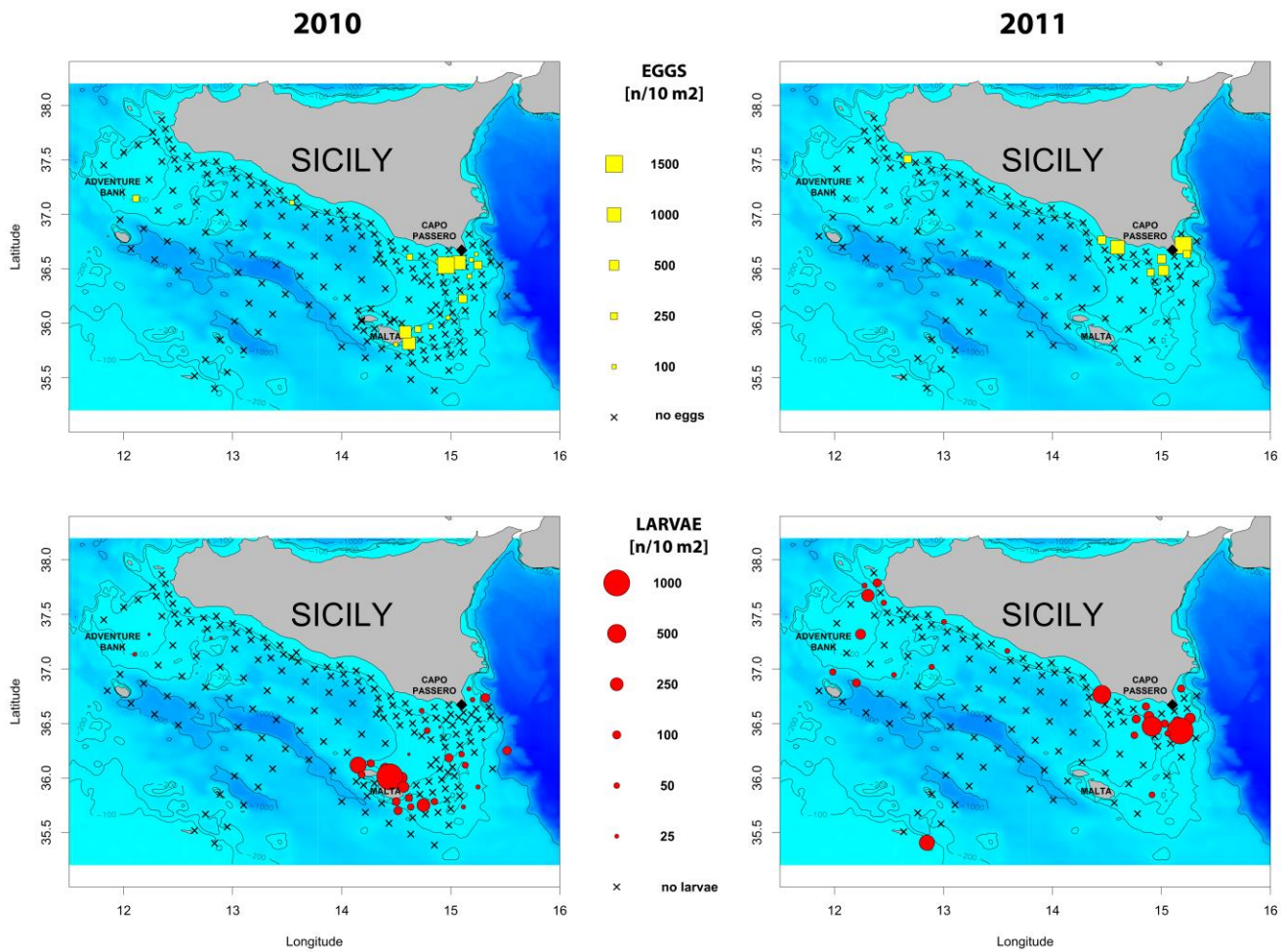
512 Zarrad, R., Missaoui, H., Alemany, F., Mohamed Salah, R., Garcia, A., Othman, J., and Abed Amor,  
513 E.: Spawning areas and larval distributions of anchovy *Engraulis encrasicolus* in relation to  
514 environmental conditions in the Gulf of Tunis (Central Mediterranean Sea). *Sci. Mar.*, 70(S2), 137-146,  
515 2006.

516

517 Table 1. Satellite products that are used in this work.  $\Delta t$  and  $\Delta x$  indicate temporal and spatial  
 518 resolutions, respectively. SST: sea surface temperature Pathfinder V5.2 (PFV52) AVHRR data  
 519 interpolated through an Optimal Interpolation algorithm (Pisano et al., 2015); Chl: sea surface  
 520 chlorophyll concentration computed by applying the MedOC4 algorithm (Volpe et al., 2007) to the  
 521 ESA-CCI remote sensing reflectance (Rrs) spectra (ESA-CCI Rrs results from the merging of  
 522 SeaWiFS, MODIS-Aqua and MERIS sensors); Ocean Wind: Cross-Calibrated, Multi-Platform Ocean  
 523 Surface Wind Velocity Product (multi-sensor, made of SeaWinds su QuikSCAT e ADEOS-II, AMSR-  
 524 E, TRMM TMI, SSM/I); ~~Sea surface geostrophic velocity: multimission altimeter products (Saral,  
 525 Cryosat 2, Jason 1&2, T/P, Envisat, GFO, ERS 1 & 2 and even Geosat).~~

Parameter	$\Delta t$	$\Delta x$	Data source
SST – Pathfinder V5.2 (PFV52) AVHRR L4 data	daily	4 × 4 km	<a href="http://www.myocean.eu.org/">http://www.myocean.eu.org/</a>
Chl – ESA-CCI-L4 data	daily	4 × 4 km	<a href="http://www.myocean.eu.org/">http://www.myocean.eu.org/</a>
Ocean Wind	daily	25 × 25 km	<a href="http://podaac.jpl.nasa.gov">http://podaac.jpl.nasa.gov</a>

526



527

528 Figure 1. Map of the study area (i.e., Sicily Channel) showing the sampling stations. Bathymetry is  
 529 indicated by contours~~are indicated contours~~ and by background colors, from cyan (shallower) to blue  
 530 (deeper). The isobaths of 100, 200 and 1000 m are shown. Red circles and yellow squares represent  
 531 larval (upper panels) and eggs (downlower panels) density of *Sardinella aurita* during 2010 (left) and  
 532 2011(right) surveys, respectively. The main points of interest are indicated (i.e., Adventure Bank,  
 533 Malta, and Capo Passero).

534

535

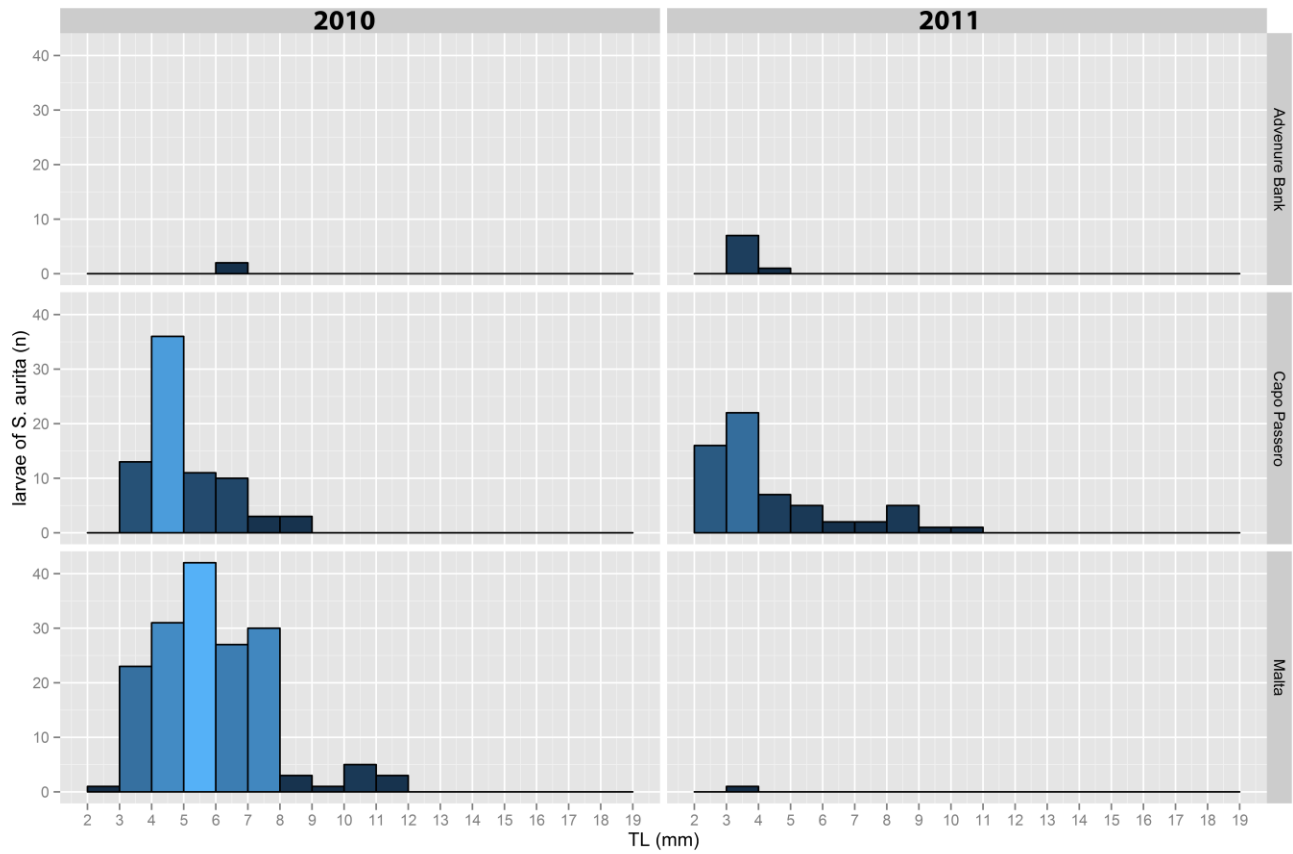
536

537

538

539

540



541

542 Figure 2. Frequency histograms of the total lengths (TLs) measured off Adventure Bank, Capo Passero,  
543 and Malta during the two Bansic 2010 and 2011 cruises.

544

545

546

547

548

549

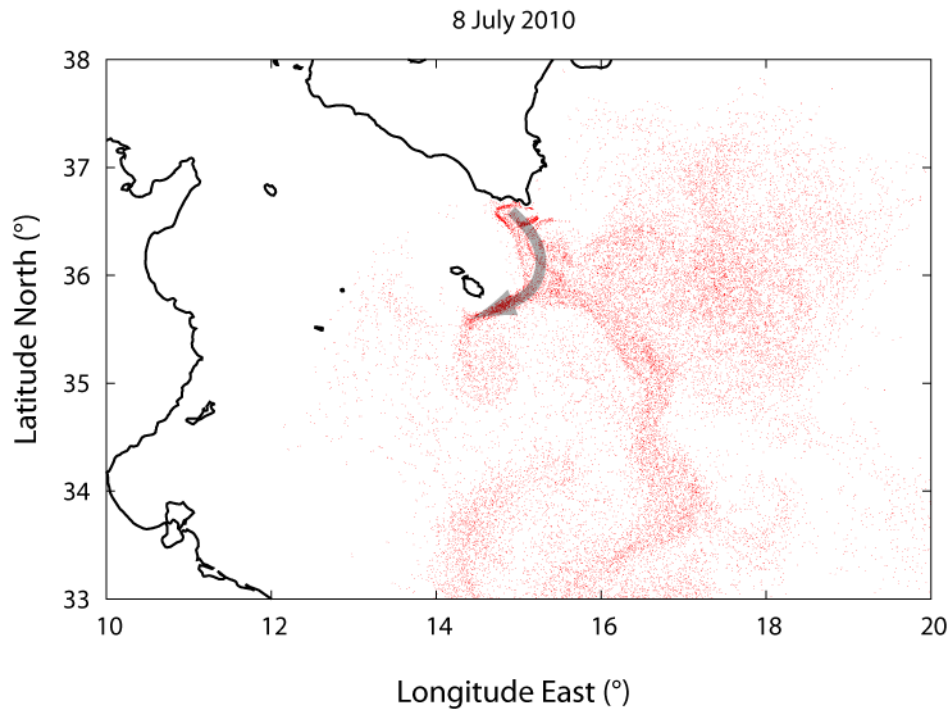
550

551

552

553

554



555

556 Figure 3. Lagrangian run snapshot on 8 July 2010 showing the net transport of *Sardinella Aurita* larvae  
557 (red dots) from Capo Passero to Malta that occurs along the cold filament forming off Capo Passero.  
558 The grey arrow highlights the net transport of larvae.

559

560

561

562

563

564

565

566

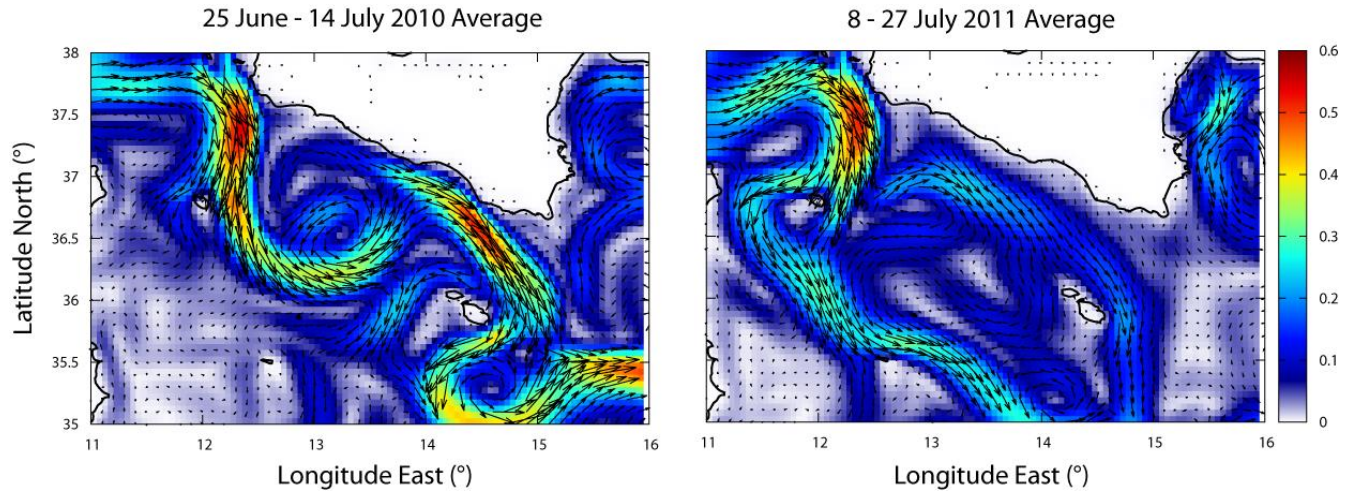
567

568

569

570

571



572

573 Figure 4. Cruise averaged Eulerian velocity fields for the two Bansic 2010 and 2011 cruises: 25 June to  
574 14 July 2010 and 8 to 27 July 2011, respectively.

575

576

577

578

579

580

581

582

583

584

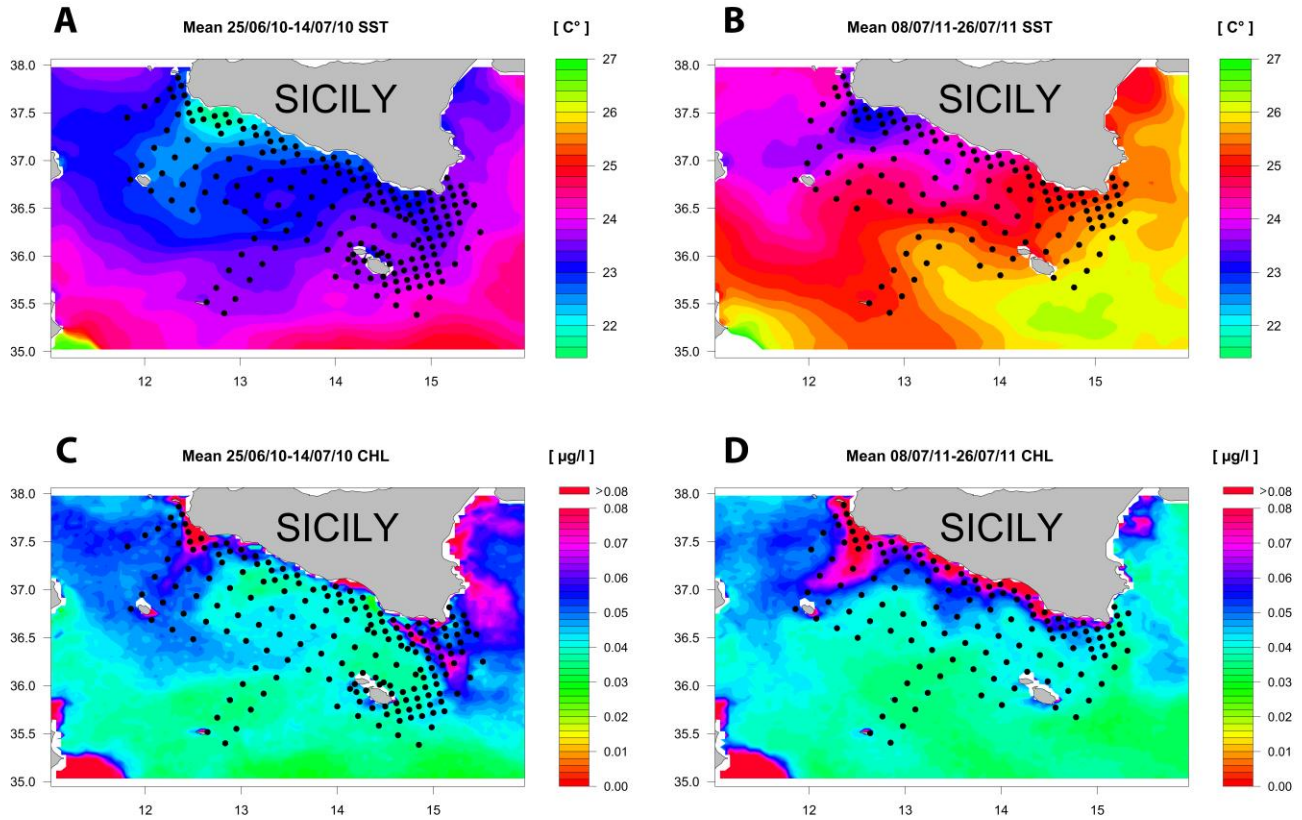
585

586

587

588

589



590

591 Figure 5. Cruise averaged Sea Surface Temperature (aA, cC) and Chlorophyll concentration (bB, dD)  
592 for the two Binsic 2010 and 2011 cruises.

593

594

595

596

597

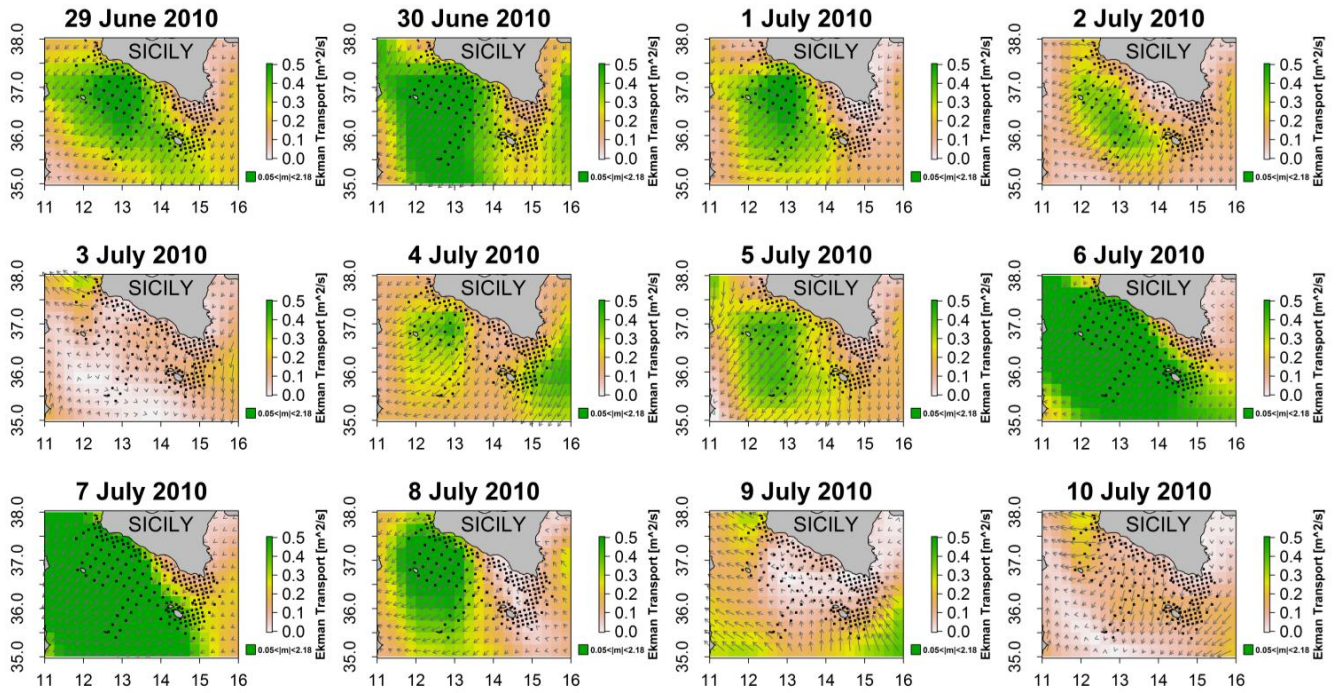
598

599

600

601





602

603 Figure 6. Daily Ekman transport during the Binsic 2010 cruise, from 29 June to 10 July.

604

605

606

607

608

609

610

611

612

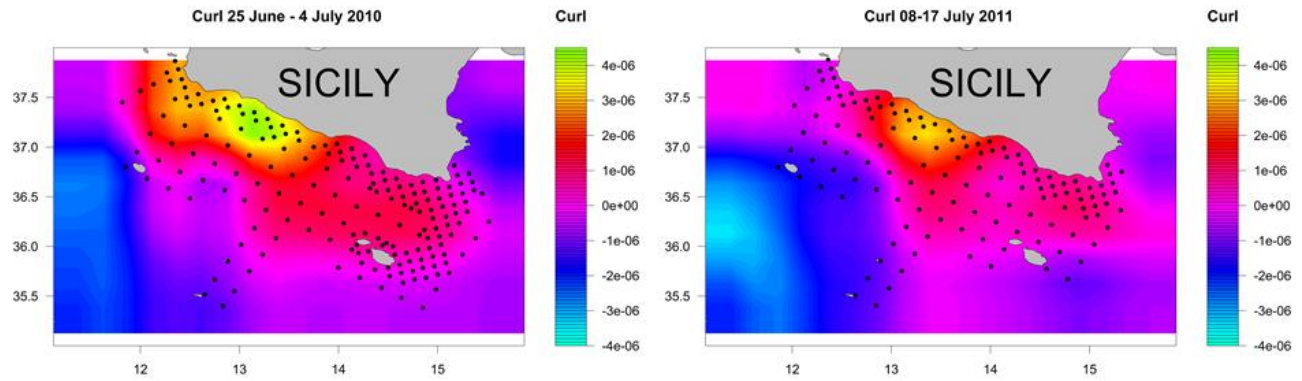
613

614

615

616

617



618

619 Figure 7. Integral of the curl of wind stress  $\rho h \Pi$  ( $\text{Ns/m}^3$ ) (see Eq. 4) performed throughout the Bansic  
 620 2010 (25 June to 14 July) and Bansic 2011 (8 to 27 July) cruises showing the more intense potential  
 621 vorticity increase that occurred in 2010. Such a potential vorticity input led to the formation-offshore  
 622 propagation of the cold filament.

623